Princeton Plasma Physics Laboratory

PPPL-4185

PPPL-4185

Fluctuations and Discrete Particle Noise in Gyrokinetic Simulation of Drift Waves

Thomas G. Jenkins and W.W. Lee

August 2006

PPPL
PRINCETON PLASMA PHYSICS LABORATORY

Prepared for the U.S. Department of Energy under Contract DE-AC02-76CH03073.

Princeton Plasma Physics Laboratory
Report Disclaimers

Full Legal Disclaimer

Trademark Disclaimer

PPPL Report Availability

Princeton Plasma Physics Laboratory

This report is posted on the U.S. Department of Energy's Princeton Plasma Physics Laboratory Publications and Reports web site in Fiscal Year 2006.

The home page for PPPL Reports and Publications is:

http://www.pppl.gov/pub_report/

Office of Scientific and Technical Information (OSTI):

Available electronically at: http://www.osti.gov/bridge.

Available for a processing fee to U.S. Department of Energy and its contractors, in paper from:

U.S. Department of Energy
Office of Scientific and Technical Information
P.O. Box 62
Oak Ridge, TN 37831-0062

Telephone: (865) 576-8401

Fax: (865) 576-5728

E-mail: reports@adonis.osti.gov

Fluctuations and discrete particle noise in gyrokinetic simulation of drift waves

Thomas G. Jenkins and W. W. Lee

Princeton Plasma Physics Laboratory

Princeton, NJ 08543

Abstract

The relevance of the gyrokinetic fluctuation-dissipation theorem (FDT) to thermal equilibrium and nonequilibrium states of the gyrokinetic plasma is explored, with particular focus being given to the contribution of the weakly damped normal modes to the fluctuation spectrum. It is found that the fluctuation energy carried in the normal modes exhibits the proper scaling with particle count (as predicted by the FDT in thermal equilibrium) even in the presence of drift waves which grow linearly and attain a nonlinearly saturated steady state. This favorable scaling is preserved, and the saturation amplitude of the drift wave unaffected, for parameter regimes in which the normal modes become strongly damped and introduce a broad spectrum of discreteness-induced background noise in frequency space. The relationship of the present work to the more general issue of discrete particle noise in particle-in-cell simulations is discussed.

I. Introduction

The gyrokinetic model of a plasma, in addition to its original success [1],[2] in analytically describing low-frequency phenomena (relative to the ion gyrofrequency) of moderate wavelength ($k_\perp \rho_i \sim 1$, where ρ_i is the ion gyroradius), has also been shown to be extremely well-suited for use in large-scale numerical simulations [3, 4]. Recent particle-in-cell (PIC) simulations [5], for instance, can use upwards of thirty billion particles on massively parallel machines, and are able to model the behavior of toroidal fusion plasmas at multiple-teraflop speeds. On more modest scales, gyrokinetic PIC simulations have been used to investigate turbulence spreading in shaped plasmas [6], collisionless and collisional tearing modes [7], and the effects of nonadiabatic electrons [8] on turbulent simulations. They have also been employed to study collisional damping of zonal flows [9], ion temperature gradient-driven turbulence in toroidal geometry [10], and the size scaling of transport parameters in turbulent plasmas [11].

Recent discussion in the fusion simulation community has centered on the topic of "discrete particle noise" and the effects that such noise may have on the long-time transport predictions of turbulent gyrokinetic PIC simulations [12], [13]. Physical effects (such as collisions) are indeed associated with the discrete nature of the particles in a plasma. The discrete particle noise we discuss here, however, is associated with collisionless plasmas; the statistical properties of the simulation and the physical plasma differ due to the comparatively small number of particles one can feasibly use in these simulations ($N \sim 10^{10} \ll 10^{23}$ particles in a typical fusion reactor). Despite this, accurate predictions for the behavior

of such plasmas can be made by PIC simulations that are based on finite-size particles [14] (eliminating the need to calculate the N^2 interparticle forces, through the modification of particle interactions inside a Debye sphere), the gyrokinetic PIC model [3] (removing the space charge waves and simplifying the gyromotion), and the δf method [15] (allowing one to model only the deviation of the plasma from a known equilibrium). Nevertheless, it is reasonable to wonder how, and to what extent, the representation of many physical particles by comparatively few computational entities affects the simulation results.

One may gain some insight into the nature of discreteness-induced noise in the plasma by examining the behavior of the fluctuation spectrum $\langle \delta\phi\delta\phi \rangle(\mathbf{k}, \omega)$. In this work, we explore the behavior of the fluctuation spectrum as low-frequency drift waves drive the plasma from thermal equilibrium to a nonlinearly saturated steady state, examining the behavior of the spectrum as a function of particle count and giving particular attention to the contribution of the weakly damped normal modes of the plasma to this spectrum. These normal modes carry the bulk of the particle discreteness-induced noise in electrostatic gyrokinetic plasmas [4], [16], [17]; we explore the validity of this statement as parameters of the system change so that the normal modes are no longer well-defined (i.e. as the damping rate of the normal modes becomes large). Additionally, we present specific results (relevant to the general issue of the relationship between noise and signal in a PIC simulation treated in existing literature [14], [18], [19]) regarding the effects of discreteness-induced noise on the long-time behavior of nonlinearly saturated drift waves.

Section II of this paper introduces the equations of the gyrokinetic model, and presents the gyrokinetic fluctuation-dissipation theorem (FDT). In section III we describe the normal modes of the gyrokinetic plasma, and explore the conditions under which they are well-defined. We demonstrate that our thermal equilibrium simulations are consistent with the theory and that these simulations satisfy the gyrokinetic FDT. Section IV explains how the simulation methods used can be generalized to include the possibility of a density gradient and linear drift waves; a calculation describing the nonlinear saturation of these waves is also given. Section V describes the relevance of the gyrokinetic FDT to the nonequilibrium, nonlinearly saturated states of the gyrokinetic plasma, and presents simulation results showing the relationship of these states and the particle-discreteness-induced background noise in the presence and absence of well-defined normal modes. We then conclude with some comments on the applicability of this work to the more general issue of the effect of noise in PIC simulations.

II. The gyrokinetic model

A. Governing equations

In the limit of $k_\perp^2 \rho_i^2 \ll 1$, the gyrokinetic Vlasov equation, which describes the phase space evolution of a gyrocenter distribution function $F_\alpha(\mathbf{x}, v_\parallel, t)$, can be written (in the absence of magnetic field gradients, and in the electrostatic limit) as

$$\frac{\partial F_\alpha}{\partial t} + v_\parallel \mathbf{b}\cdot\nabla F_\alpha - \nabla\phi\times\mathbf{b}\cdot\nabla F_\alpha - \frac{q_\alpha m_i}{q_i m_\alpha}\mathbf{b}\cdot\nabla\phi\frac{\partial F_\alpha}{\partial v_\parallel} = 0\ . \tag{1}$$

This equation, which resembles the drift kinetic equation, uses the conventional gyrokinetic normalization; lengths and times are normalized to the scaled gyroradius $\rho_s \equiv \sqrt{T_e/m_i}/\Omega_i$ and the inverse ion cyclotron frequency $\Omega_i^{-1} = (q_i B_0/m_i)^{-1}$, while the electrostatic potential ϕ is normalized to the electron temperature $T_e/|q_e|$. Here $\mathbf{b}$ is a unit vector in the direction of the (uniform) magnetic field $\mathbf{B} = B_0\mathbf{b}$, and $v_\parallel$ is a velocity coordinate parallel to this field. The charge, mass, and temperature of species α are represented by q_α, m_α, and T_α respectively, and we assume that the ions are singly charged ($q_i = |q_e|$).

The gyrokinetic Poisson equation, in these normalized units, is given by

$$\nabla^2\phi\left(\frac{\lambda_{De}^2}{\rho_s^2}\right) + \nabla_\perp^2\phi = -\sum_\alpha \frac{q_\alpha}{q_i}\int_{-\infty}^{\infty} F_\alpha dv_\parallel \tag{2}$$

with the first term on the left arising from the conventional Laplacian operator in Poisson's equation and the second term arising from the polarization charge [3]. Because the electron Debye length $\lambda_{De} = (\epsilon_0 T_e/n_0 q_e^2)^{1/2}$ is much smaller than ρ_s, the first of these terms may be neglected. The dominance of the polarization term in Eq. (2) effectively changes the fundamental length scale of the gyrokinetic plasma from λ_{De} to ρ_s; we will later see this effect in examining the low-frequency limit of the gyrokinetic dielectric function.

For our slab model, we postulate a magnetic field in the $\mathbf{b} = \theta\hat{y} + \hat{z}$ direction (for some $\theta \ll 1$). We ignore variation in the $\hat{z}$ direction, and study

the evolution of waves (perpendicular to the dominant field component) with discrete wavenumbers $\mathbf{k} \equiv k_x l\hat{x} + k_y m\hat{y}$, for integer l and m, with $k_x \equiv 2\pi/L_x$ and $k_y \equiv 2\pi/L_y$. Here L_x and L_y are the dimensions of the slab (using periodic boundary conditions) in the $\hat{x}$ and $\hat{y}$ directions. We can then define a fundamental parallel wavenumber $k_\parallel \equiv \theta k_y$ and the perpendicular wavenumber $k_\perp(l,m) = \sqrt{k^2 - m^2 k_\parallel^2}$.

These equations are solved by the standard PIC methods, initially loading a set of particles with some reasonable initial conditions (in our case, a Maxwellian distribution in $v_\parallel$ and a uniform distribution in $\mathbf{x}$). We then iteratively evolve the positions of these particles according to the characteristics of the gyrokinetic Vlasov equation, interpolate their positions to a spatial grid, and calculate the electrostatic potential using Fourier transforms.

B. The fluctuation-dissipation theorem

In thermal equilibrium, and in the absence of spatial gradients, the linear dielectric function relevant to the physical system of Eqs. (1) and (2) can be written as

$$\mathcal{D}_{l,m}(\omega) = 1 + \frac{X_i + X_e}{k_\perp^2(l,m)} \; . \tag{3}$$

Here, $X_\alpha \equiv 1 + \xi_\alpha Z(\xi_\alpha)$, where $\xi_\alpha = \omega/\sqrt{2} m k_\parallel v_{t\alpha}$ and Z is the plasma dispersion function. The thermal velocity is given (because of the gyrokinetic normalization) by $v_{t\alpha} = \sqrt{m_i T_\alpha / m_\alpha T_e}$, and the dispersion relation can be obtained from the zeros of $\mathcal{D}_{l,m}(\omega)$. In the limit as $\omega \to 0$, the dielectric function (apart from a change of characteristic scale length $\lambda_{De} \to \rho_s$) describes the

familiar Debye shielding effect of kinetic theory.

The resemblance of Eqs. (1) and (2) to the conventional Vlasov-Poisson system suggests that many parallels can be drawn between gyrokinetic and conventional Vlasov theory, and Krommes *et al.* [17] have initially treated this topic (see also Ref. [20] for a lengthier discussion), formulating the classical fluctuation-dissipation theorem for a gyrokinetic plasma in the electrostatic approximation. According to the theorem, the thermal equilibrium fluctuation spectrum of our slab model satisfies

$$\langle \delta\phi\delta\phi\rangle_{l,m}(\omega) = \frac{2}{N\omega k_\perp^2(l,m)}\mathrm{Im}\left(1 - \frac{1}{\mathcal{D}_{l,m}(\omega)}\right) \ . \tag{4}$$

Integration of this formula over all frequencies using residue theory, and normalizing to 2π, yields the fluctuation spectrum as a function of wavenumber only,

$$\langle \delta\phi\delta\phi\rangle_{l,m} = \frac{1}{T}\int_0^T \langle|\phi_{l,m}(t)|^2\rangle dt = \frac{1}{Nk_\perp^2(l,m)[1 + k_\perp^2(l,m)/2]} \ , \tag{5}$$

where T is the time over which the simulation runs (the left hand side being the time-averaged $|\phi_{l,m}(t)|^2$) and N is the number of particles of a given species.

III. Normal modes

A. Theory

In certain cases [21], the dominant contributions to Eq. (4) come from only a few localized peaks at various values of ω in the spectrum. If we consider the case of normal modes (oscillations which damp on a timescale slow compared to the period of the wave), we can separate the real and imaginary parts of the dielectric function, $\mathcal{D}_{l,m}(\omega) = \mathcal{D}'_{l,m}(\omega) + i\mathcal{D}''_{l,m}(\omega)$, and obtain

$$\mathrm{Im}\left(1 - \frac{1}{\mathcal{D}_{l,m}(\omega)}\right) = \left[\frac{\mathcal{D}''_{l,m}(\omega)}{\mathcal{D}'_{l,m}(\omega)^2 + \mathcal{D}''_{l,m}(\omega)^2}\right] . \tag{6}$$

In the limit of small $\mathcal{D}''_{l,m}(\omega)$, which we expect from a normal mode, this Lorentzian form reduces to

$$\mathrm{Im}\left(1 - \frac{1}{\mathcal{D}_{l,m}(\omega)}\right) = \pi\delta(\mathcal{D}'_{l,m}(\omega)) = \pi\sum_{p=1}^{p_0} \frac{\delta(\omega - \omega_p)}{\left(\partial\mathcal{D}'_{l,m}(\omega)/\partial\omega\Big|_{\omega=\omega_p}\right.} \tag{7}$$

where we have assumed that there are p_0 normal modes (i.e. solutions of $\mathcal{D}'_{l,m}(\omega_p) = 0$ for which the denominator is nonsingular). Consequently, we can write the approximate relation

$$\langle\delta\phi\delta\phi\rangle_{l,m}(\omega) = \frac{2\pi}{Nk_\perp^2(l,m)}\sum_{p=1}^{p_0} \frac{\delta(\omega - \omega_p)}{\omega\left(\partial\mathcal{D}'_{l,m}(\omega)/\partial\omega\Big|_{\omega=\omega_p}\right.} . \tag{8}$$

This implies that the bulk of the fluctuation energy for a given wavenumber,

as a function of ω, resides in localized peaks about the real frequencies of the normal modes, if such modes can be reasonably well-defined.

The plasma described by the linear dielectric of Eq. (3) has two normal modes which are conventionally referred to as ω_H-modes [4]; with the appropriate changes of scaling, these modes are analogous to the well-known Langmuir waves of conventional Vlasov theory in the long-wavelength limit. If we assume the ion and electron thermal velocities are small relative to the resonant phase velocity $\omega/k_\parallel$, we can expand $Z(\xi_\alpha)$ to obtain

$$\mathcal{D}'_{l,m}(\omega) \approx 1 - \frac{\omega_H^2}{\omega^2} \quad ; \quad \omega_H^2 = \frac{m^2 k_\parallel^2 (v_{te}^2 + v_{ti}^2)}{k_\perp^2(l,m)} \quad ; \quad \omega_r = \pm|\omega_H| \; . \tag{9}$$

This gives the approximate result

$$\langle \delta\phi\delta\phi \rangle_{l,m}(\omega)|_{\text{large } \omega} \approx \frac{2\pi}{N k_\perp^2(l,m)} \left[\frac{\delta(\omega - \omega_H)}{2} + \frac{\delta(\omega + \omega_H)}{2} \right] \tag{10}$$

for the fluctuation spectrum at high frequencies.

The existence of these normal modes depends on the system size L_y through the parallel wavenumber $k_\parallel$. As the system size decreases, the resonant phase velocity moves from the tail of the initial Maxwellian distribution into the bulk of the distribution, the damping rate increases (as is the case for Langmuir waves, where the damping rate is proportional to the slope of the background distribution at the resonant velocity), and it is no longer meaningful to speak of the disturbance as a wave (it damps away on a timescale similar to the period of the real oscillation frequency). Additionally, the approximation of

the Lorentzian of Eq. (6) as a delta function begins to fail; the distinct real frequency of a mode with long parallel wavelength is replaced by a band of frequencies near ω_r. Thus, for larger parallel wavenumbers, the energy in the fluctuation spectrum cannot be said to reside in "normal modes"; rather, it resides in random fluctuations excited by the discrete nature of the particles in the plasma.

Ion acoustic modes may also be normal modes of Eq. (3); in the limit $\xi_e \ll 1, \xi_i \gg 1$; letting $\xi_e \sim 0$ and expanding $Z(\xi_i)$ to lowest nontrivial order yields

$$\mathcal{D}'_{l,m}(\omega) \approx \frac{[1-k_\perp^2(l,m)]}{k_\perp^2(l,m)}\left(1-\frac{\omega_{IA}^2}{\omega^2}\right) \quad ; \quad \omega_{IA}^2 = \frac{m^2 k_\parallel^2 v_{ti}^2}{[1+k_\perp^2(l,m)]} \quad ; \quad \omega_r = \pm|\omega_{IA}| \tag{11}$$

for intermediate values of ω ($k_\parallel v_{ti} \ll \omega \ll k_\parallel v_{te}$). However, these modes (as were the ω_H-modes for small parallel wavelengths) are strongly Landau damped in thermal equilibrium; their effects are relatively unimportant if the ω_H-modes are well-defined. The delta-function approximation (integrating only over intermediate values of ω) is consistent with this result; we obtain

$$\langle\delta\phi\delta\phi\rangle_{l,m}(\omega)|_{\text{int. }\omega} \approx \frac{2\pi}{N}\frac{1}{[1+k_\perp^2(l,m)]}\left[\frac{\delta(\omega-\omega_{IA})}{2}+\frac{\delta(\omega+\omega_{IA})}{2}\right] . \tag{12}$$

Since $k_\perp^2 \ll 1$, the coefficient multiplying the delta-functions is significantly smaller for these modes than the corresponding coefficient in Eq. (10).

It is known from Eq. (5) that integrating the exact fluctuation spectrum over all frequencies (normalized to 2π) yields the result

$$\langle \delta\phi\delta\phi\rangle_{l,m} \text{ exact} = \frac{1}{Nk_\perp^2(l,m)[1+k_\perp^2(l,m)/2]} = \frac{1}{Nk_\perp^2(l,m)} - \frac{1}{N[2+k_\perp^2(l,m)]} \tag{13}$$

which ought to be well-matched by the sum of the ω-integrals over the approximate spectra we have derived in Eqs. (10) and (12). Performing these integrals and normalizing to 2π, we find that our procedure slightly overestimates the correct answer; we obtain

$$\langle \delta\phi\delta\phi\rangle_{l,m} \text{ approx.} = \frac{1}{Nk_\perp^2(l,m)} + \frac{1}{N[1+k_\perp^2(l,m)]} \tag{14}$$

with the first term coming from the ω_H modes and the second from the ion acoustic modes. However, it is clear that the delta-function approximation is reasonable; the error is on the order of the relative contribution of the ion acoustic modes, which is small.

B. Numerical simulations

With our knowledge of the thermal equilibrium fluctuation spectra, we now verify that our code satisfies the fluctuation-dissipation theorem. We evolve particles along the characteristics of the gyrokinetic Vlasov equation, Eq. (1), obtaining

$$\frac{dx_{\alpha j}}{dt} = -\left(\left.\frac{\partial\phi}{\partial y}\right|_{\mathbf{x}=\mathbf{x}_{\alpha j}}\right. \quad ; \quad \frac{dy_{\alpha j}}{dt} = v_{\parallel \alpha j}\theta + \left(\left.\frac{\partial\phi}{\partial x}\right|_{\mathbf{x}=\mathbf{x}_{\alpha j}}\right.$$

$$\frac{dv_{\parallel \alpha j}}{dt} = -\frac{q_\alpha m_i}{q_i m_\alpha}\theta\left(\left.\frac{\partial\phi}{\partial y}\right|_{\mathbf{x}=\mathbf{x}_{\alpha j}}\right. . \tag{15}$$

We also utilize the standard δf technique of setting $F_\alpha = F_{0\alpha} + \delta f_\alpha$ in Eq. (1); perturbations around the background Maxwellian $F_{0\alpha}$ are examined by defining the particle weight $w_\alpha \equiv \delta f_\alpha / F_\alpha$ and evolving the resulting weight equation

$$\frac{dw_{\alpha j}}{dt} = -(1 - w_{\alpha j}) v_{\parallel \alpha j}\theta\frac{q_\alpha}{q_i}\left(\left.\frac{\partial\phi}{\partial y}\right|_{\mathbf{x}=\mathbf{x}_{\alpha j}}\right. \tag{16}$$

along with Eqs. (15). The appropriately weighted density perturbations are then interpolated to a grid and the potential found via Fourier transforms.

Numerically, one can also directly solve Eq. (3) and obtain a representation of Eq. (4) as a function of ω for a given (l, m). Normalizing this representation to $2\pi\langle\delta\phi\delta\phi\rangle_{l,m}$ [from Eq. (5)], we can then qualitatively compare the results with the predictions of Eqs. (10) and (12) and our simulations. As expected, we observe in Figs. 1 and 2 that the power does indeed reside in localized peaks which spread as the parallel wavenumber grows, and that the ion acoustic modes are relatively unimportant for small parallel wavenumbers. Here we have used $L_x = 32$, $\theta = 0.01$, $(l, m) = (1, 1)$, and $v_{te}^2 = m_i/m_e \approx 1837.0$ as L_y assumes the values $[30, 23, 16]$, yielding $k_\perp \rho_i = [0.08, 0.11, 0.19]$ respectively. The simulations use 128 gridpoints in both the x and y directions, along with $N = 250,000$ particles and a timestep $\Delta t = 0.1$). One notes that the positions of the peaks in

ω are not well matched by our delta-function approximation; however, this can be rectified by retaining more terms in the expansion of the plasma dispersion functions (the algebra is unduly complicated and will not be included here). As previously mentioned, one can also see the degradation of the delta-function approximation of Eq. (7) (as well as the increasing contribution of the ion acoustic modes to the spectrum) as the parallel wavenumber is increased.

As noted by Hu and Krommes [22], the use of the δf method requires us to normalize the potential fluctuations by a typical weight $\bar{w}$. For the ω_H-modes, which (as the disparate velocities of Eq. (9) suggest) are predominantly supported by the electrons, the natural choice for $\bar{w}$ in this case is the root-mean-square electron weight $\sqrt{\sum_{j=1}^{N} w_{ej}(t)^2/N}$. We exhibit the simulation results, along with the theoretical curve obtained from Eq. (5) at lowest order, in Fig. 3. The simulation uses 128 gridpoints in the x and y directions, with $L_x = L_y = 23$ and timestep $\Delta t = 0.0125$. The parallel field component is given by $\theta = 0.01$, and we have $T_e = T_i = 1$ and $m_i/m_e = 1837.0$; only the $(l, m) = (\pm 1, \pm 1)$ Fourier components of the potential are retained. The agreement is quite good, even with an average of less than one marker particle per species per grid cell ($N \sim 1.6 \times 10^4$ in the figure).

IV. Drift modes

A. Linear growth

We now relax the constraint of thermal equilibrium by introducing a background density gradient which gives rise to drift waves. It is common [15, 23, 24] to impose a fixed background density gradient by modeling the particle density as an x-dependent function of a parameter κ_N, such that

$$\nabla F_{0\alpha} = -\kappa_N F_{0\alpha} \tag{17}$$

and neglecting this x-dependence where the gradient does not act specifically on $F_{0\alpha}$. Generally, we must have $|\kappa_N| < k_x$ for this procedure to be valid (though this restriction is unnecessary for modes propagating perpendicular to the density gradient). With this assumption, the gyrokinetic Vlasov and Poisson equations (assuming equal temperatures for ions and electrons) can be written in the δf formalism as

$$\begin{aligned} &\frac{\partial \delta f_\alpha}{\partial t} + v_\parallel \theta \frac{\partial \delta f_\alpha}{\partial y} + \kappa_N \frac{\partial \phi}{\partial y} F_{0\alpha} + v_\parallel \theta \frac{q_\alpha}{q_i} \frac{\partial \phi}{\partial y} F_{0\alpha} \\ &-\nabla\phi \times \hat{z} \cdot \nabla \delta f_\alpha - \frac{q_\alpha m_i}{q_i m_e} \theta \frac{\partial \phi}{\partial y} \frac{\partial \delta f_\alpha}{\partial v_\parallel} = 0 \ , \end{aligned} \tag{18}$$

$$\nabla_\perp^2 \phi = -\sum_\alpha \frac{q_\alpha}{q_i} \int_{-\infty}^{\infty} \delta f_\alpha dv_\parallel \ . \tag{19}$$

We now make a standard assumption of quasilinear theory [25], namely that

(for real $\omega_{l,m}$),

$$\phi(x,y,t) = \sum_{l=-\infty}^{\infty} \sum_{m=-\infty}^{\infty} \hat{\phi}_{l,m}(\epsilon t) e^{ik_x lx} e^{ik_y my} e^{-i\omega_{l,m} t} \tag{20}$$

$$\delta f_\alpha(x,y,v_\parallel,t) = \sum_{l=-\infty}^{\infty} \sum_{m=-\infty}^{\infty} \widehat{\delta f}_{\alpha,l,m}(v_\parallel,\epsilon t) e^{ik_x lx} e^{ik_y my} e^{-i\omega_{l,m} t} \tag{21}$$

where the quantities $\hat{\phi}_{l,m}(\epsilon t)$ and $\widehat{\delta f}_{\alpha,l,m}(v_\parallel,\epsilon t)$ vary slowly in time relative to the period $T = 2\pi/\omega_{l,m}$. Defining $\omega_N^* \equiv k_y \kappa_N$, we then obtain

$$\frac{\partial}{\partial t}\widehat{\delta f}_{\alpha,l,m}(v_\parallel,\epsilon t) - i(\omega_{l,m} - mk_\parallel v_\parallel)\widehat{\delta f}_{\alpha,l,m}(v_\parallel,\epsilon t)$$

$$+ im\hat{\phi}_{l,m}(\epsilon t) F_{0\alpha}(v_\parallel) \left(\omega_N^* + \frac{q_\alpha}{q_i} k_\parallel v_\parallel\right) + \sum_{l'=-\infty}^{\infty} \sum_{m'=-\infty}^{\infty} e^{i(\omega_{l,m} - \omega_{l',m'} - \omega_{l-l',m-m'})t}$$

$$\left[k_x k_y (m'l - l'm) - im' k_\parallel \frac{q_\alpha m_i}{q_i m_e} \frac{\partial}{\partial v_\parallel}\right] \hat{\phi}_{l',m'}(\epsilon t) \widehat{\delta f}_{\alpha,l-l',m-m'}(v_\parallel,\epsilon t) = 0 \tag{22}$$

$$-k_\perp^2(l,m)\hat{\phi}_{l,m}(\epsilon t) = -\sum_\alpha \frac{q_\alpha}{q_i} \int_{-\infty}^{\infty} \widehat{\delta f}_{\alpha,l,m}(v_\parallel,\epsilon t) dv_\parallel \tag{23}$$

Ignoring the nonlinear $\hat{\phi}_{l',m'}(\epsilon t)\widehat{\delta f}_{\alpha,l-l',m-m'}(v_\parallel,\epsilon t)$ terms allows us to solve the Vlasov equation,

$$\widehat{\delta f}_{\alpha,l,m}(v_\parallel,\epsilon t) = \widehat{\delta f}_{\alpha,l,m}(v_\parallel,0) e^{i(\omega_{l,m} - mk_\parallel v_\parallel)t}$$

$$-imF_{0\alpha}(v_\parallel)\left(\omega_N^* + \frac{q_\alpha}{q_i} k_\parallel v_\parallel\right) \int_0^t \hat{\phi}_{l,m}[\epsilon(t-\lambda)] e^{i(\omega_{l,m} - mk_\parallel v_\parallel)\lambda} d\lambda \ . \tag{24}$$

If we then let $\hat{\phi}_{l,m}[\epsilon(t-\lambda)] \approx \hat{\phi}_{l,m}(\epsilon t) e^{-\lambda\gamma_{l,m}}$ (an assumption appropriate

both for the Landau-damped normal modes and the drift modes, where $\gamma_{l,m}$ is the damping/growth rate), we obtain (after some algebra) the linear expression

$$\widehat{\delta f}_{\alpha,l,m}(v_\parallel,\epsilon t)=\frac{mF_{0\alpha}(v_\parallel)\left(\omega_N^*+\frac{q_\alpha}{q_i}k_\parallel v_\parallel\right)\hat{\phi}_{l,m}(\epsilon t)}{\omega_{l,m}-mk_\parallel v_\parallel+i\gamma_{l,m}} \tag{25}$$

and the linear dispersion relation

$$0=k_\perp^2(l,m)-\sum_\alpha\left(1+\frac{mq_\alpha}{q_i}\frac{\omega_N^*}{\omega_{l,m}+i\gamma_{l,m}}\right)\int_{-\infty}^{\infty}\frac{mk_\parallel v_\parallel F_{0\alpha}(v_\parallel)}{\omega_{l,m}-mk_\parallel v_\parallel+i\gamma_{l,m}}dv_\parallel\ . \tag{26}$$

From the latter equation we can recover the drift wave by assuming that the resonant phase velocity is much larger than the ion thermal speed (so that ion terms may be neglected altogether) and much less than the electron thermal speed; the assumption that $\gamma_{l,m}\ll\omega_{l,m}$ then yields

$$0=k_\perp^2(l,m)+1-\frac{m\omega_N^*}{\omega_{l,m}+i\gamma_{l,m}}+\frac{i\sqrt{\pi}(\omega_{l,m}-m\omega_N^*)\gamma_{l,m}}{\sqrt{2}mk_\parallel v_{te}|\gamma_{l,m}|} \tag{27}$$

with solution

$$\omega_{l,m}=\frac{m\omega_N^*}{1+k_\perp^2(l,m)}\ \ ;\ \ |\gamma_{l,m}|=\frac{\sqrt{\pi}m^2\omega_N^{*2}k_\perp^2(l,m)}{(1+k_\perp^2(l,m))^3\sqrt{2}mk_\parallel v_{te}}\ . \tag{28}$$

One observes that $\omega_{l,m}=-\omega_{l,-m}=-\omega_{-l,-m}$ and that the drift modes grow (or damp) independently of the sign of l or m. Consequently, Eq. (25) can be used to show that $\hat{\phi}_{l,-m}^*(\epsilon t)=\hat{\phi}_{l,m}(\epsilon t)$.

B. Nonlinear saturation

Because of the nonlinear terms in Eq. (22), the drift waves described by Eq. (26) which grow in time will eventually saturate. We can examine this saturation mechanism in a simple case by restricting the potential to modes of one particular wavenumber ($l = \pm 1, m = \pm 1$) and ignoring the parallel velocity nonlinearity [the velocity derivatives in Eq. (22)]. Our approach is very similar to the mode coupling calculation of Lee *et al.* [26], and an analogous derivation (in the 1-dimensional case) has been carried out by Parker and Lee [15]. The equation for ($l = 2, m = 0$) is given by

$$\frac{\partial}{\partial t}\delta f_{\alpha,2,0}(v_\parallel,\epsilon t) - i\omega_{2,0}\delta f_{\alpha,2,0}(v_\parallel,\epsilon t)$$

$$+2k_xk_ye^{i\omega_{2,0}t}\left[\hat{\phi}_{1,1}(\epsilon t)\widehat{\delta f}_{\alpha,1,-1}(v_\parallel,\epsilon t) - \hat{\phi}_{1,-1}(\epsilon t)\widehat{\delta f}_{\alpha,1,1}(v_\parallel,\epsilon t)\right] = 0 \qquad (29)$$

which forces $\omega_{2,0} = 0$. Substitution of the linear values for $\widehat{\delta f}_{\alpha,1,\pm 1}(v_\parallel,\epsilon t)$ then yields the nonlinear result

$$\widehat{\delta f}_{\alpha,2,0}(v_\parallel,\epsilon t) = -\frac{2\pi i k_x k_y F_{0\alpha}(v_\parallel)\hat{\phi}_{1,1}(\epsilon t)\hat{\phi}_{1,-1}(\epsilon t)}{\gamma_{1,1}}\left(\omega_N^* + \frac{q_\alpha}{q_i}k_\parallel v_\parallel\right)\delta(\omega_{1,1} - k_\parallel v_\parallel)\,. \qquad (30)$$

A similar procedure for $l = 0, m = 2$ yields no contribution, so we can then write the nonlinear equation for ($l = 1, m = 1$);

$$\frac{\partial}{\partial t}\widehat{\delta f}_{\alpha,1,1}(v_\parallel,\epsilon t)-i(\omega_{1,1}-k_\parallel v_\parallel)\widehat{\delta f}_{\alpha,1,1}(v_\parallel,\epsilon t)+i\hat{\phi}_{1,1}(\epsilon t)F_{0\alpha}(v_\parallel)\left(\omega_N^*+\frac{q_\alpha}{q_i}k_\parallel v_\parallel\right)$$

$$+2k_xk_y\hat{\phi}^*_{1,-1}(\epsilon t)\widehat{\delta f}_{\alpha,2,0}(v_\parallel,\epsilon t)=0 \tag{31}$$

with approximate solution

$$\widehat{\delta f}^{NL}_{\alpha,1,1}=\frac{F_{0\alpha}(v_\parallel)\left(\omega_N^*+\frac{q_\alpha}{q_i}k_\parallel v_\parallel\right)\hat{\phi}_{1,1}(\epsilon t)}{\omega_{1,1}-k_\parallel v_\parallel+i\gamma_{1,1}}\left[1-\frac{4k_x^2k_y^2\pi}{\gamma}|\hat{\phi}_{1,-1}(\epsilon t)|^2\delta(\omega_{1,1}-k_\parallel v_\parallel)\right]. \tag{32}$$

When this result is inserted into the Poisson equation and the drift-wave dispersion relation calculated, we obtain

$$0=k_\perp^2(1,1)+1-\frac{\omega_N^*}{\omega_{1,1}+i\gamma_{1,1}}+\frac{i\sqrt{\pi}(\omega_{1,1}-\omega_N^*)}{\sqrt{2}k_\parallel v_{te}}\left[1-\frac{4k_x^2k_y^2|\hat{\phi}_{1,-1}(\epsilon t)|^2}{\gamma_{1,1}^2}\right]. \tag{33}$$

The real part of the frequency is unchanged, but saturation occurs when the potential grows such that the imaginary term is zero;

$$|\hat{\phi}_{1,\pm1}(\epsilon t)|\approx\frac{\gamma_{1,1}}{2k_xk_y} \tag{34}$$

in agreement with the calculation of Ref. [26] (and noting that $\hat{\phi}_{1,1}=\hat{\phi}^*_{1,-1}$). Comparing this result with our simulations, we find that this procedure slightly underestimates the saturation level, as Fig. 4 shows. Nevertheless, one can

plausibly argue (both analytically and from the data) that nonlinear effects do indeed cause the mode to saturate, and it is the existence of such a saturation mechanism (rather than the detailed description of it) that we will primarily make use of in the remainder of this paper.

V. Saturated states and the FDT

If we include a density gradient in the background distribution, the dielectric function in Eq. (3) generalizes to

$$\mathcal{D}_{l,m}(\omega) = 1 + \frac{X_i}{k_\perp^2(l,m)}\left(1 + \frac{m\omega_N^*}{\omega}\right) + \frac{X_e}{k_\perp^2(l,m)}\left(1 - \frac{m\omega_N^*}{\omega}\right) \ . \qquad (35)$$

The introduction of a density gradient as a free energy source necessarily implies that the system is no longer in thermal equilibrium, so one cannot apply the fluctuation-dissipation theorem directly without careful consideration. It is plausible, however, that the theorem can be applied to a nonlinearly saturated system containing only damped and marginally stable modes when the deviation from thermal equilibrium is small. For the nonlinearly saturated drift waves we have simulated, we know from Eq. (28) that the real frequency of the drift wave, which scales as ω_N^*, is well separated from the high-frequency components of the fluctuation spectrum (arising from the interaction of the density gradient with the low-frequency ion acoustic wave). Even when this background gradient is large enough to amplify these low-frequency fluctuations and produce unstable

drift waves, our simple model for the saturation mechanism predicts a negligible shift in the real frequency of the mode. Low-frequency fluctuations are amplified by the density gradient, grow, and nonlinearly saturate, but their energy remains in the low-frequency portion of the spectrum (as demonstrated in the previous section), well separated from and having negligible effects on the high frequency modes where the discreteness-induced noise resides. Consequently, it remains feasible to use the FDT to predict the behavior of the high-frequency portion of the spectrum.

As before, we can find the ω_H-modes by taking the limit of the dielectric function as $\xi_e, \xi_i \gg 1$, obtaining

$$\mathcal{D}_{l,m}(\omega) \approx 1 - \frac{\omega_H^2}{\omega^2} + \frac{m\omega_N^* \omega_H^2}{\omega^3} \quad ; \quad \omega_H^2 \approx \frac{k_\parallel^2 m^2 v_{te}^2}{k_\perp^2(l,m)} \; . \tag{36}$$

Because we assume ω_N^* is small, we can neglect it and recover the result of Eq. (10). Integrating the latter result only over the high frequencies, we see that the fluctuation energy in the normal modes should continue to scale inversely as the number of particles [as in Eq. (14)].

If we attempt to apply Eq. (8) to the portion of the spectrum containing the drift wave, the dispersion relation (assuming a nonlinear saturation of the general form described previously) is given by

$$\mathcal{D}_{l,m}(\omega) \approx \frac{1 + k_\perp^2(l,m)}{k_\perp^2(l,m)} \left(1 - \frac{\omega_{l,m}}{\omega} + i \frac{\omega_{l,m}\delta}{\omega^2} \right) \tag{37}$$

where δ goes to zero as the system saturates nonlinearly and $\omega_{l,m}$ is given by

Eq. (28). In this case, Eq. (8) suggests that for the drift waves,

$$\langle \delta\phi\delta\phi\rangle_{l,m}(\omega)|_{\text{small }\omega} = \frac{2\pi}{N[1+k_\perp^2(l,m)]}\delta(\omega-\omega_{l,m}) \ . \tag{38}$$

Because drift waves arise when ion acoustic waves are destabilized by a density gradient, the resemblance of this equation to Eq. (12) is reasonable. Although additional physical effects that this equation does not capture may arise (e.g. linearly growing drift modes), it is reasonable to assume (as our simulations suggest) that the prediction of Eq. (12) regarding the scaling of the discrete particle noise with N is relevant in the presence of the drift wave as well; the physics governing the linear growth and saturation of drift modes is contained even in collisionless kinetic models [e.g. the quasilinear model of Eq. (34)] and is consequently unrelated to particle discreteness. A simple estimate of the low-frequency discreteness-induced fluctuation level [the square root of the frequency integral of Eq. (38)] yields a much smaller amplitude (on the order of 3% for typical simulation parameters used in this section) than the quasilinear saturation level of Eq. (34). The attainment of a nonlinearly saturated steady state by the drift wave suggests that it may be of interest to determine whether more general equations [akin to Eqs. (10) and (38)] can be constructed to describe low-frequency discreteness-induced fluctuations about this steady state. A brief discussion on the possibility of developing an FDT for nonthermal equilibria is presented in Ref. [27]; the effects of discreteness-induced noise in such plasmas are also addressed by Kadomtsev [28]). Although we do not pursue it here, the possibility of obtaining further information about the noise by cal-

culating fluctuations about a nonlinearly saturated steady state is potentially interesting.

Turning to our data, we observe that the physical process described by the numerically obtained spectrum is not merely fluctuations at the real frequency of the drift wave, but the nonlinear saturation of these fluctuations as they are amplified by the density gradient. This saturation amplitude must be independent of the number of particles in the simulation; thus, if the code has converged, we should expect the fluctuation spectrum to exhibit a large peak at $\omega = \omega_{l,m}$ with amplitude independent of N. As well, the spectrum should contain peaks at the normal mode frequencies $\omega = \pm\omega_H$ with amplitudes which decrease inversely with N. Figure 5 confirms that this is indeed the case; these simulations use $\omega_N^* = 0.055$ and $\Delta t = 0.125$ while varying the particle count ($N = [3.2 \times 10^4, 5.0 \times 10^5, 1.0 \times 10^6]$). The other system parameters are given by $L_x = L_y = 23, \theta = 0.01, v_{te}^2 = 1837.0$, and $T_e/T_i = 1$ (as in Fig. 3). It should be mentioned here that the spatially-averaged δf_α is much smaller than the equilibrium distribution function $F_{0\alpha}$ near the phase velocity of the wave; we show this effect in Fig. 6 for the electrons. Thus, the deviation from equilibrium in the steady state is indeed small.

Some insight into the effects of discrete particle noise can be obtained by studying the behavior of Fig. 5 as the damping rate of the normal modes increases (this can be done by reducing the size of the slab in the y-direction). As we have previously noted, the concept of "normal modes" is not well-defined for large damping rate. As random fluctuations Landau damp away on timescales

increasingly near the period of the real oscillation of the "wave", the energy in these fluctuations begins to spread from a single real frequency (that of the original normal mode) to a broad band in frequency space, essentially creating a background of incoherent noise. Running simulations to investigate the effects of this broad-spectrum noise, we find that even when the normal modes of a system are not well-defined, the fluctuation spectrum still predicts the correct saturation amplitude (independent of particle count) for the drift wave while preserving the favorable scaling of the noise with particle count across the remainder of the spectrum. Figure 7 shows this effect; for these simulations we have set $L_y = 12$ and left the other system parameters unchanged from Fig. 5. It is noteworthy that while the normal mode fluctuations are well-separated from the growing drift mode in the spectra of Fig. 5, the broad, noisy band of discreteness-induced fluctuations in the top portion of Fig. 7 has spread to encompass the frequency of the drift mode (because of the low particle count). Nevertheless, this overlapping (in frequency space) of incoherent noise and (small-amplitude) coherent drift fluctuations has no appreciable effect on the saturation amplitude of the drift mode; the amplitude remains constant as the increasing particle count reduces the discrete particle noise at the drift frequency to negligible values. One might wonder about the validity of this result if the saturation amplitude were much lower than the amplitude of the incoherent noise; such a case might arise for weakly unstable drift modes [recall that the saturation amplitude scales as the growth rate, as in Eq. (34)]. However, in particle simulations the amplitude of the noise can always be reduced by using

more simulation particles, and convergence studies can be used to discern when the contribution of the noise has become negligible. The number of particles needed to guarantee this in these simulations is, in fact, quite small (less than two particles per cell).

Because we have only retained the $(\pm 1, \pm 1)$ Fourier components of the potential in our earlier simulations (effectively removing coupling terms between short-wavelength and long-wavelength modes), it is of interest to assess the effects of mode coupling on our conclusions. In general, we find that the long-term behavior of the saturated drift modes we have considered is not substantially affected by the presence of shorter-wavelength modes in the system. We consider an elongated slab with simulation parameters $L_x = 95.0, L_y = 9.5, \theta = 0.01, v_{te}^2 = 1837.0, T_e/T_i = 1$, and $\omega_N^* = 0.043$ with $N = 1,048,572$ particles and $N_x \times N_y = 256 \times 64$ gridpoints, and use the four-point averaging method of Ref. [29] to retain full gyroradius effects. This elongated geometry bears some resemblance to experimentally observed plasmas in tokamaks, with variation in x and y corresponding to radial and poloidal variation (and the $(0, 1)$ mode we study corresponding to a radial streamer). As shown in Fig. 8, although the initial transition from linear growth to saturation is affected by the presence of other modes, the long-time behavior of the $(0, 1)$ mode amplitude is not substantially affected. Though the signal is somewhat noisier when more modes are retained, this can be easily dealt with by using more particles in the simulation.

VI. Conclusions

We have shown that when the normal modes (ω_H-modes) of the gyrokinetic plasma are well-defined, the fluctuation energy carried by these modes scales inversely as the number of simulation particles even in the presence of saturated low-frequency drift instabilities. Although such instabilities are driven when the plasma is not in thermal equilibrium, one may nevertheless appeal to the fluctuation-dissipation theorem to plausibly explain this effect; the power in the fluctuation spectrum (in thermal equilibrium) is contained in high-frequency normal mode fluctuations, but the introduction of a mild density gradient excites fluctuations only at frequencies substantially lower than those of the normal modes. These fluctuations are amplified (by the free energy of the background gradient) until they saturate nonlinearly, maintaining the plasma in a marginally stable, nonequilibrium state.

Interestingly, the favorable scaling (with particle count) of the fluctuation energy external to the drift wave is preserved even when the normal modes are not well-defined and are replaced by a broad spectrum of incoherent, particle-discreteness-induced noise not well separated from the drift wave. Further, the long-time behavior of the saturated drift modes is not substantially affected by mode coupling. We surmise from our results that in many cases, the effects of discrete particle noise on PIC simulations of microturbulence are negligible (or can easily be made so) even when relatively modest numbers of simulation particles are used, in agreement with the general conclusions of Kadomtsev [28]. We also believe that the results pertaining to discrete particle noise we have

described here have relevance to the more general case of microturbulence in tokamak geometry [13].

Acknowledgments

This work is supported by U. S. Department of Energy Contract No. DE-AC02-76-CHO-3073 and the SciDAC Center for Gyrokinetic Particle Simulations of Turbulent Transport in Burning Plasmas. One of us (TGJ) would like to acknowledge useful discussions with Dr. John Krommes.

References

[1] P. Rutherford and E. A. Frieman, Phys. Fluids **11**, 569 (1968).

[2] J. B. Taylor and R. J. Hastie, Plasma Phys. **10**, 479 (1968).

[3] W. W. Lee, Phys. Fluids **26**, 556 (1983).

[4] W. W. Lee, J. Comp. Phys. **72**, 243 (1987).

[5] W. W. Lee, S. Ethier et al, SciDAC 2006, Journal of Phys: Conference Series (to appear, 2006).

[6] W. X. Wang, Z. Lin, W. M. Tang, W. W. Lee, S. Ethier, J. L. V. Lewandowski, G. Rewoldt, T. S. Hahm, and J. Manickam, Phys. Plasmas, to appear (2006).

[7] W. Wan, Y. Chen, and S. E. Parker, Phys. Plasmas **12**, 012311 (2005).

[8] Y. Chen and S. E. Parker, Phys. Plasmas **8**, 2095 (2001).

[9] Z. Lin, T. S. Hahm, W. W. Lee, W. M. Tang, and R. B. White, Phys. Plasmas **7**, 1857 (2000).

[10] S. E. Parker, W. W. Lee, and R. A. Santoro, Phys. Rev. Lett. **71**, 2042 (1993).

[11] Z. Lin, S. Ethier, T. S. Hahm, and W. M. Tang, Phys. Rev. Lett. **88**, 195004 (2002).

[12] W. M. Nevins, G. W. Hammett, A. M. Dimits, W. Dorland, and D. E. Shumaker, Phys. Plasmas **12**, 122305.

[13] Z. Lin, L. Chen, and F. Zonca, Phys. Plasmas **12**, 056125 (2005).

[14] A. B. Langdon and C. K. Birdsall, Phys. Fluids **13**, 2115 (1970).

[15] S. E. Parker and W. W. Lee, Phys. Fluids B **5**, 77 (1993).

[16] W. W. Lee, J. L. V. Lewandowski, T. S. Hahm, and Z. Lin, Phys. Plasmas **8**, 4435 (2001).

[17] J. A. Krommes, W. W. Lee, and C. Oberman, Phys. Fluids **29**, 2421 (1986).

[18] A. B. Langdon, Phys. Fluids **22**, 163 (1979).

[19] C. K. Birdsall and A. B. Langdon, *Plasma Physics via Computer Simulation* (McGraw-Hill, New York, 1985).

[20] J. A. Krommes, Phys. Fluids B **5**, 1066 (1993).

[21] Y. L. Klimontovoch, *The Statistical Theory of Non-Equilibrium Processes in a Plasma* (MIT, Cambridge, 1967).

[22] G. Hu and J. A. Krommes, Phys. Plasmas **1**, 863 (1994).

[23] I. Manuilskiy and W. W. Lee, Phys. Plasmas **7**, 1381 (2000).

[24] J. A. Krommes and G. Hu, Phys. Plasmas **1**, 3211 (1994).

[25] A. N. Kaufman, J. Plasma Physics **8**, 1 (1972).

[26] W. W. Lee, J. A. Krommes, C. R. Oberman, and R. A. Smith, Phys. Fluids **27**, 2652 (1984).

[27] G. Bekefi, *Radiation Processes in Plasmas* (Wiley, New York, 1966), pp. 126-130.

[28] B. B. Kadomtsev, *Plasma Turbulence* (Academic Press, London, 1965), pp. 44-46.

[29] W. W. Lee and H. Qin, Phys. Plasmas **10**, 3196 (2003).

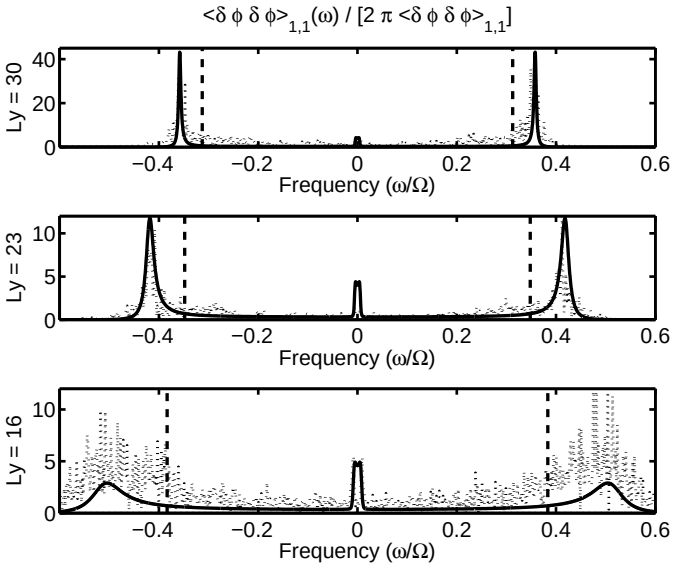

Figure 1: The normalized fluctuation spectrum $\langle\delta\phi\delta\phi\rangle_{l,m}(\omega)/[2\pi\langle\delta\phi\delta\phi\rangle_{l,m}]$ for $(l,m) = (1,1)$ from the numerical solution of Eq. (4) (solid lines) and our simulation results (dotted lines) are plotted together with the delta-function approximation of Eq. (10) for the ω_H-modes (dashed lines) as the parallel component of the wavelength is varied.

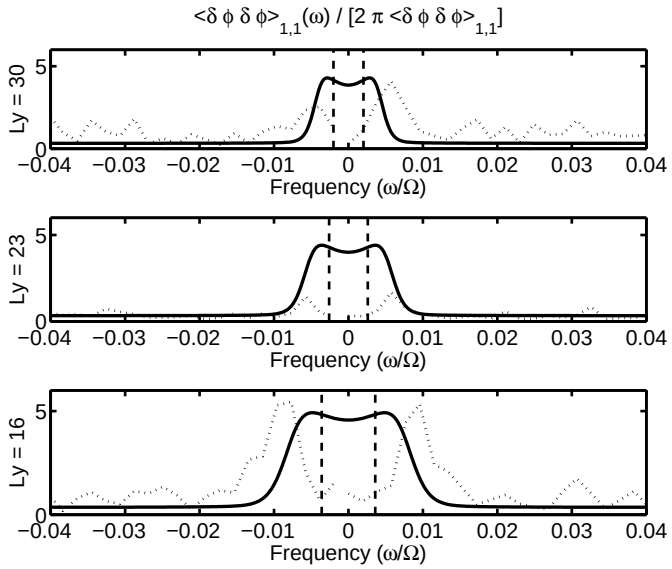

Figure 2: The simulation results and theoretical predictions of Fig. 1, together with the delta-function approximation of Eq. (12) for the ion acoustic modes (dashed lines), are plotted over a narrower frequency range as the parallel component of the wavelength is varied.

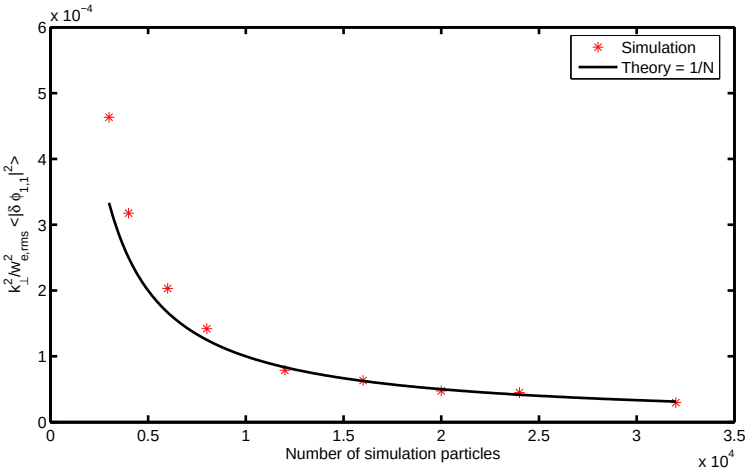

Figure 3: Simulation results and theory exhibiting the scaling of the ω-integrated fluctuation spectrum with the number of simulation particles. The theoretical curve is obtained from Eq. (5) in the $k_\perp^2(l,m) \ll 1$ limit, with the potential normalized to the root-mean-square electron weight.

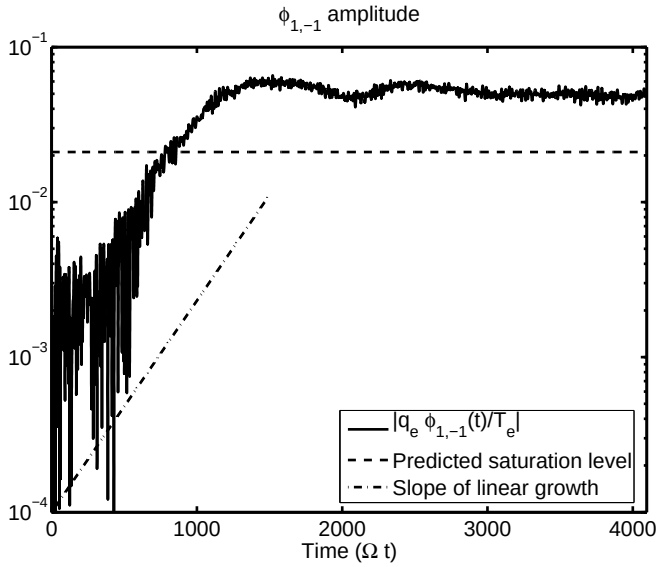

Figure 4: The nonlinearly saturated $\phi_{1,-1}(t)$ mode amplitude and the quasilinear prediction of Eq. (34) for the saturation level, together with the expected growth rate from linear theory (only the slope of the line is meaningful). The simulation uses the same parameters as Fig. 3.

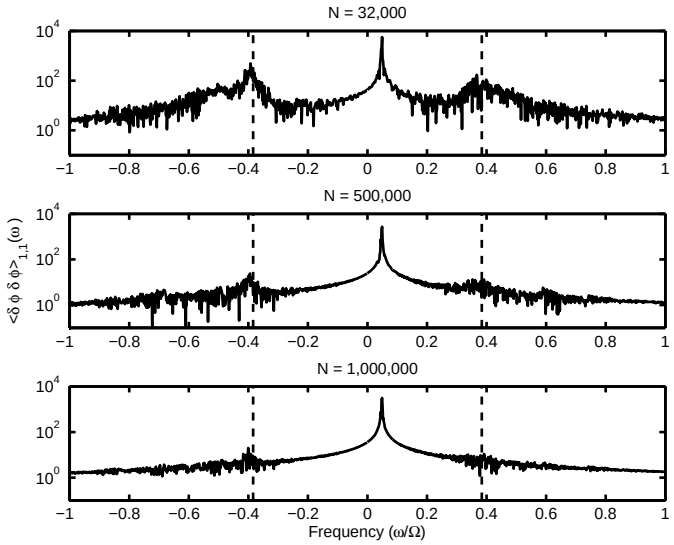

Figure 5: As the number of particles in the simulation is increased, the saturation amplitude of the drift wave remains constant while the amplitude of the spectral noise carried by the ω_H modes (whose real frequencies are indicated by dashed lines) decreases.

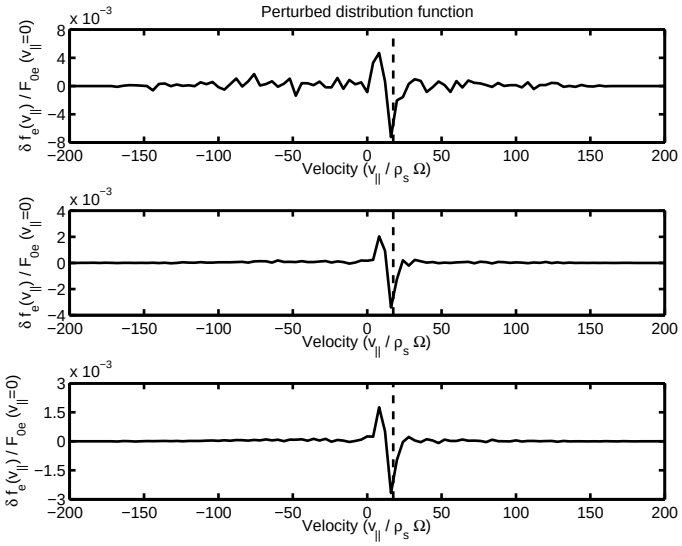

Figure 6: The spatial average of the perturbed distribution function δf_e, normalized to the value $F_{0e}(v_\parallel = 0)$ (where F_{0e} is the background Maxwellian) for the three simulations of Fig. 5. The resonant phase velocity of the drift wave is indicated by the dashed lines.

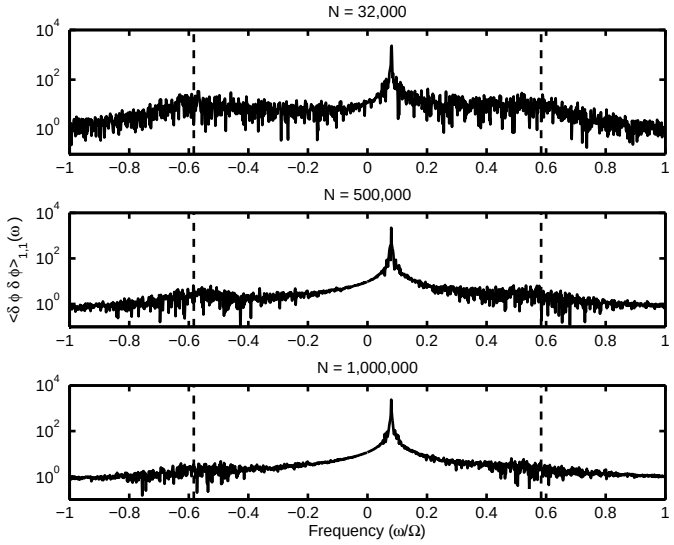

Figure 7: In the absence of clearly defined normal modes (with the real frequency of the strongly damped ω_H-mode indicated by dashed lines), the broad spectrum of background noise overlaps the portion of the spectrum occupied by the growing drift wave at low N. Nevertheless, the noise amplitude does not appreciably affect the saturation amplitude of this wave, and favorable scaling of the noise amplitude is obtained as the particle count is raised.

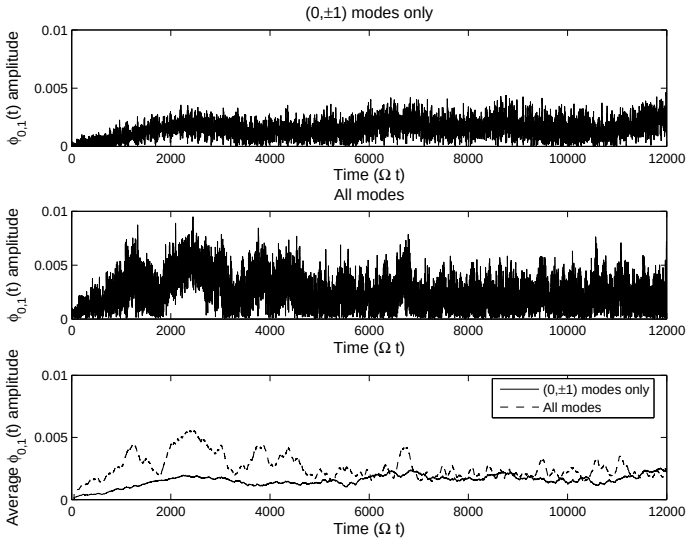

Figure 8: The long-time behavior of $\phi_{0,1}(t)$ is shown for an elongated simulation with $L_x = 95.0, L_y = 9.5$. Only the $(0, \pm 1)$ components of the potential have been retained in the top curve; the simulation shown in the middle plot retains all the modes. A running average over several periods of the high-frequency noise is taken below, showing that mode coupling does not substantially affect the long-time behavior of the saturated drift mode.

The Princeton Plasma Physics Laboratory is operated
by Princeton University under contract
with the U.S. Department of Energy.

Information Services
Princeton Plasma Physics Laboratory
P.O. Box 451
Princeton, NJ 08543

Phone: 609-243-2750
Fax: 609-243-2751
e-mail: pppl_info@pppl.gov
Internet Address: http://www.pppl.gov